The real structure of the Si_6 cluster

Aristides D. Zdetsis
Department of Physics, University of Patras, Patras, GR 26500, Greece
(Received 10 September 1999; revised manuscript received 4 January 2001; published 12 July 2001)

Contrary to well-established recent theoretical results based on second-order Moller-Plesset perturbation theory, it is illustrated here that the distorted octahedron of D_{4h} symmetry cannot be the ground state of the ''magic'' Si_6 cluster, but a transition state, connecting two almost isoenergetic structures of lower symmetry, which can coexist. This conclusion, the consequences of which could be far reaching for other magic clusters, is based on higher-order perturbation theory, accurate coupled-cluster CCSD(T) calculations and density-functional theory at the hybrid B3LYP level. The discrepancy is due to the poor convergence of the perturbation expansion, related to the flatness of the energy hypersurface near the minimum. As a result, the structural and electronic properties of Si_6 are still not well understood, although several suggestions are put forward here.

DOI: 10.1103/PhysRevA.64.023202 PACS number(s): 36.40.−c, 31.15.Ew, 61.46.+w, 73.22.−f

I. INTRODUCTION

Small and medium-size silicon clusters containing up to 100 atoms have been studied extensively both experimentally and theoretically due to their scientific and technological importance [1–8]. However, several questions still remain open, especially about bonding and structural properties, for which comparison between experimental and theoretical results is only indirect even for moderate-size clusters. On the other hand, small clusters such as Si_6, for which a wealth of experimental and theoretical results exist [4,5], are considered as fully and well understood.

Si_6 is one of several very important ''magic'' clusters, the characteristics of which have been used extensively to model and parametrize much larger systems through empirical and semiempirical calculations. The currently accepted ground state of Si_6 is a distorted octahedron shown in Fig. 1(a), predicted by geometry optimization using second-order Moller-Plesset perturbation theory (MP2) calculations [5]. However, earlier calculations [4], based on Hartree-Fock (HF) gradients, had led to an edge-capped trigonal bipyramid of C_{2v} symmetry as the ground state, shown in Fig. 1(c). Above this state there is a very close-lying bicapped tetrahedron, which can also be viewed as a face-capped trigonal bipyramid of near C_{2v} symmetry. This last structure, initially of C_{2v} symmetry, was unstable to distortions and was finally stabilized by further geometry optimization into the C_s symmetric structure of Fig. 1(b). Both of these structures [Figs. 1(a) and 1(b)] on MP2 optimization collapse to the same distorted octahedron structure of D_{4h} symmetry [Fig. 1(a)].

On the experimental side, the measured Raman spectrum [5] seems to provide indirect support to the MP2 predictions. The MP2 calculated spectrum for the D_{4h} structure, after a 5% scaling, is in quite good agreement with experiment. In spite of this, the present results, which are based on higher-order perturbation theory as well as density-functional theory (DFT) in hybrid schemes such as the well-known B3LYP [9,10], do not agree with the MP2 predictions. The present results, which show that all three structures in Fig. 1 are essentially isoenergetic, are further supported by higher-level coupled-cluster calculations with all single and double substitutions and a quasiperturbative estimate of the effect of triple excitations, CCSD(T).

The resulting discrepancy is rather surprising since Si_6, unlike the majority of other small and medium-size clusters, is widely considered as a well-established system, almost a textbook case, both theoretically and experimentally. However, a deeper understanding of this rather negative finding could turn out to be a very positive starting point for a better comprehension of the ''magic'' property.

II. SOME TECHNICAL DETAILS

The bulk of the present calculations was carried out using the GAUSSIAN 94 program package [11]. Various initial structures were chosen for full geometry optimization under a given symmetry, starting with octahedral symmetry. Following the optimization under O_h symmetry, the optimization was further continued under subgroups of O_h such as D_{4h}, D_{3d}, D_{2h}, C_{2v}, and C_s. The real local minima among the resulting stationary points were identified (a) by continuing

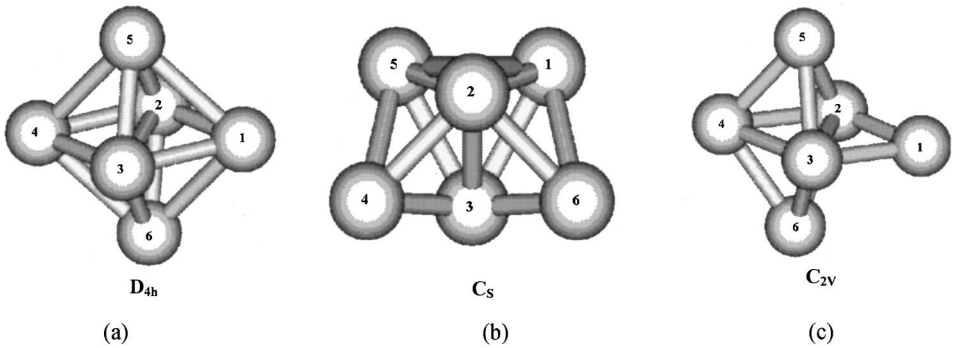

FIG. 1. The three structures competing for the ground state of the Si_6 cluster.

TABLE I. Comparative energies of the low-lying Si_6 structures relative to the C_s isomer. The quoted values of energy correspond to B3LYP geometry and to the 6-31G* basis set. For the D_{4h} structure the energies at the MP2 geometry are given in parentheses. The absolute value of the B3LYP energy for the C_s structure is −1736.896 119 72 atomic units. The MP2 and CCSD(T) energy values of the C_s structure are listed in Table II below.

Symmetry of the structure	ΔE (kcal/mole) MP2	CCSD(T)	B3LYP
D_{3d}	+35.3		+31.6
D_{3d} triplet	+30.0	+28.5	+23.2
D_{4h} triplet	+20.9	+19.3	+15.5
D_{4h}	−1.0 (−1.5)	+1.2 (+1.0)	+1.0
C_{2v}	+1.0	+0.4	+0.0
C_s	0.0	0.0	0.0

the optimization without any symmetry restrictions (C_1 symmetry), and (b) by vibrational analysis, checking for possible imaginary values.

In addition to the 6-31G* atomic basis set, the larger D95* basis set was used. For the DFT/B3LYP calculations, the even larger cc-pVDZ correlation-consistent basis set was also employed. The results obtained with these larger basis sets fully confirm those obtained with the 6-31G* basis set. For space economy and consistency with the calculations of Ref. [5], the discussion will be focused here on the results obtained with the 6-31G* basis set. Some key results obtained with the D95* basis set [11], however, will also be presented for comparison (in Table III below).

III. RESULTS AND DISCUSSION

As we can see in Table I, the three structures in Figs. 1(a), 1(b), and 1(c), which are topologically different with D_{4h}, C_s, and C_{2v} symmetries, respectively, lie very close in energy, competing for the ground state at various levels of theory. It is clear from Table I that the remaining isomers (such as the D_{3d} symmetric hexagonal chair, in both singlet and triplet electronic configurations, and the triplet configuration of the D_{4h} structure) need not be considered further here since they are much higher in energy.

The disagreement of the MP2 with the CCSD(T) and DFT/B3LYP results that is revealed in Table I implies that MP2 and, more generally, the perturbational approach could be questionable for this system. This is confirmed by Table II, which shows in addition the energies of the three competing structures at the level of HF and third-(MP3) and fourth-(MP4SDTQ) order Moller-Plesset perturbation theory, together with coupled-cluster CCSD and CCSD(T) results. The MPFSDTQ results include singles (S), doubles (D), triples (T), and quadruples (Q) contributions. The same results obtained with the larger D95* basis set are given in Table III for comparison.

In both of these tables we can see that the energy differences involved are extremely small. The energy differences between all three isomers are of the order of 0.1 kcal/mole (the difference between C_{2v} and C_s is smaller than 0.1 kcal/mole, and between C_s and D_{4h} 1 kcal/mole at the 6-31G* level and about 0.1 kcal/mole at the D95* level). In spite of these extremely small differences, we can see in Table II that the D_{4h} structure is the lowest in energy only at the MP2 level. At the HF, MP3, MP4SDTQ, CCSD, and CCSD(T) levels of theory it is higher than the other two. Table III illustrates that this picture is preserved with the larger D95* basis set, with even smaller differences between the three structures, which eventually must be isoenergetic. It is clear that the oscillations of the relative energies at different levels of correlation and orders of perturbation theory are comparatively small, but nevertheless very significant. Such oscillations were observed earlier in the Si_{10} cluster [6,7], where the magnitude of the relative energy oscillations was significantly larger. For Si_{10} the HF geometry was used for the evaluation of the higher-order terms, whereas in the present calculation the MP2 and B3LYP optimized geometries are used. This could be the reason for the smaller magnitude of the oscillations.

Since vibrational frequencies are very sensitive to even small energy differences, we have also performed vibrational analysis, with some results shown in Table IV, for all three structures at MP2, MP3, MP4, and B3LYP levels. This, in addition, tests whether or not these structures are true local minima of the energy hypersurface, by checking for possible imaginary frequencies.

The C_{2v} structure of Fig. 1(b), which is completely analogous to the edge-capped trigonal bipyramid of Raghavachari's earlier work [4], is a true local minimum at the

TABLE II. Absolute energies in atomic units (6-31G* basis set). The energies in the first three columns correspond to the B3LYP optimized geometry, while the fourth column gives the energies of the D_{4h} structure at the MP2 optimized geometry.

	Structure			
Method	C_s	C_{2v}	D_{4h}	D_{4h}/MP2
HF	−1733.360 551	−1733.360 679	−1733.354 206	−1733.354 710
MP2	−1733.931 275	−1733.929 716	−1733.932 939	−1733.933 733
MP3	−1733.917 838	−1733.917 543	−1733.916 229	−1733.916 229
MP4SDTQ	−1734.001 835	−1734.000 550	−1734.001 572	−1734.001 579
CCSD	−1733.932 769	−1733.932 240	−1733.931 700	−1733.930 998
CCSD(T)	−1733.982 118	−1733.981 508	−1733.980 1816	−1733.980 490
State	$^1A'$	$^1A_1$	$^1A_{1g}$	$^1A_{1g}$

TABLE III. Absolute energies in atomic units using the D95* basis set. The energies of the C_s and C_{2v} structures, as in Table II, correspond to the B3LYP optimized geometry. The energies of the D_{4h} structure are given at the MP2 optimized geometry.

	Structure		
Method	C_s	C_{2v}	D_{4h}
HF	−1733.383 962	−1733.384 411	−1733.381 269
MP2	−1733.989 200	−1733.988 409	−1733.990 781
MP3	−1733.972 622	−1733.972 747	−1733.971 587
MP4SDTQ	−1734.063 381	−1734.062 753	−1734.062 809
CCSD	−1733.987 462	−1733.987 404	−1733.986 721
CCSD(T)	−1734.040 527	−1734.040 374	−1734.040 007
State	$^1A'$	$^1A_1$	$^1A_{1g}$

B3LYP (and HF) level. At the MP2 level it collapses, under geometry optimization, to the distorted octahedron of Fig. 1(a).

The bicapped tetrahedron of Fig. 1(b), known also as the face-capped trigonal bipyramid from Raghavachari's earlier work [4], was initially obtained by geometry optimization under C_{2v} symmetry restrictions. The resulting C_{2v} structure was not a true local minimum of the energy hypersurface, as was revealed by the existence of one imaginary frequency of b_2 symmetry. Reoptimization of this structure (at the B3LYP level) after distortion according to the b_2 displacements led to the C_s symmetric structure of Fig. 1(b). This structure, which has near C_{2v} symmetry, at the MP2 level also transforms into the D_{4h} structure, similarly to the structure of Fig. 1(b).

Finally, the Jahn-Teller distorted octahedron of D_{4h} symmetry, which is the established ground state according to Honea *et al.* [5], is indeed a local minimum at the MP2 level. However, at both MP3 and MP4 as well as the B3LYP levels it has two degenerate E_u modes with imaginary frequencies (even at the MP2 level this mode is very soft). This indicates that a lower-symmetry structure might be more stable. Distorting the D_{4h} structure according to one of the displacement patterns of this vibrational mode results in transformation to the edge-capped trigonal bipyramid of Fig. 1(c), under geometry optimization at the MP3 or B3LYP levels. The displacement patterns of the first E_u mode are shown in Fig. 2(b). In Figs. 2(a) and 2(c), respectively, the starting and ending geometries of the optimization are also shown. As we can see in Fig. 2, this mode pushes atoms 5 and 6 away from atom 1 while at the same time it pulls atoms 2 and 3 toward it. The ending structure is the C_{2v} structure of Fig. 1(c) analogous to the edge-capped trigonal bipyramid of Raghavachari [4], from which it can also be obtained through direct MP3 or B3LYP geometry optimization. Similarly, the second degenerate E_u mode transforms the D_{4h} structure into the near C_{2v} structure of Fig. 1(b). Thus, according to MP3, MP4, and B3LYP, the D_{4h} isomer is a transition state, connecting the structures in Figs. 1(b) and 1(c). This state can lead through the displacement patterns of the imaginary frequencies to the lower-symmetry C_{2v} and C_s states. At the MP2 level the opposite happens: both C_s and C_{2v} structures transform into the D_{4h} structure. Apparently the higher-order MP3 and MP4 calculations and the B3LYP results present the correct picture, which is further supported by CCSD(T) energy calculations.

The theoretical interpretation in Ref. [5] was based on MP2 calculations, which as we see in Table IV are identical with our MP2 results after scaling by 5%. The scaled MP2 results of Table IV show an overall good agreement with the measured Raman frequencies. This has been considered [5] as indirect support of the MP2 results. The MP3, MP4, and B3LYP results (without any arbitrary scaling) for the D_{4h} structure agree quite well with the experimental measurements and the MP2 results for the Raman-active modes. For the odd-parity modes (E_u, B_{2u}, and A_{2u}) however, there are substantial differences between the MP2 results on one hand and the MP3, MP4, and B3LYP predictions on the other

TABLE IV. Vibrational properties of the Si_6 D_{4h} isomer at various levels of theoretical treatment. Some "corresponding" frequencies are also given for the C_{2v} and C_s structures. Frequencies are given in cm^{-1}. The symbol *i* indicates imaginary frequencies.

		D_{4h}					C_{2v}	C_s
Experimental frequencies Ref. [5]	Symmetry assignment	MP2 scaled by 5% Ref. [5]	MP2 no scaling (this work)	MP3 no scaling (this work)	MP4SDQ no scaling (this work)	B3LYP no scaling (this work)	B3LYP no scaling (this work)	B3LYP no scaling (this work)
	E_u		52	81*i*	75*i*	79*i*		
	B_{2u}		197	117	149	117		
252	B_{2g}	209	220	252	225	234	276	276
300	A_{1g}	298	314	331	319	312	295	295
	A_{2u}		358	344	347	315		
386	B_{1g}	376	396	418	404	386	361	360
404	E_g	425	447	424	421	395	395	370
458	A_{1g}	457	481	480	476	442	436 460	439 448 451
	E_u		482	483	480	443		

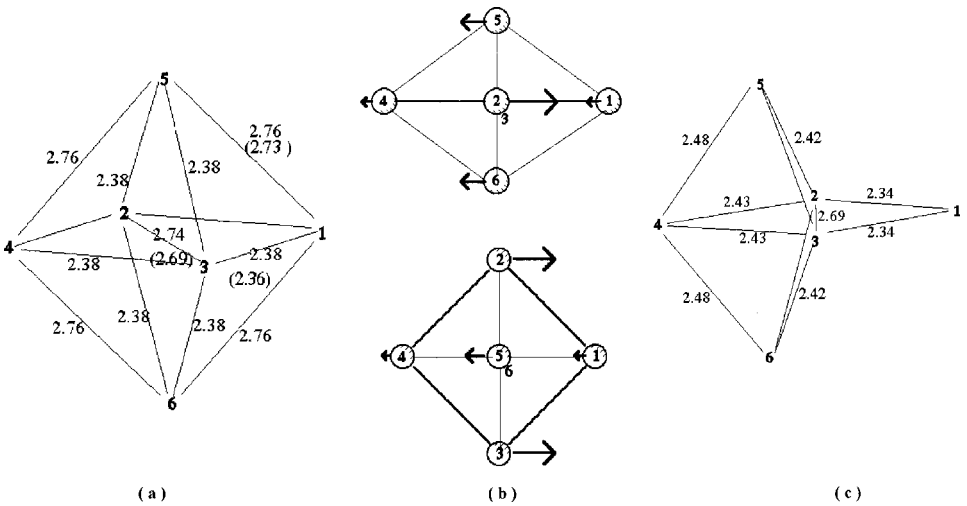

FIG. 2. Transformation of the D_{4h} distorted tetrahedron: the structure (a), according to the displacements patterns of the first E_u mode (b), into the edge-capped trigonal bipyramid (c). The bond lengths in (a) and (c) are in angstroms and correspond to the B3LYP optimized geometry. The MP2 bond lengths are given in parentheses. The displacement vectors in (b) are given in the plane defined by the atoms 1, 4, 5, and 6 (top), and in the plane of the atoms 1, 2, 4, and 5 (bottom).

hand, which could be checked by infrared spectroscopy. The most striking difference has to do with the MP2 soft E_u mode at 52 cm^{-1}, which at the MP3 and B3LYP levels turns unstable with an imaginary frequency, thus revealing that the D_{4h} structure is not a true local minimum of the energy hypersurface but a transition state.

On the other hand, the C_{2v} and C_s structures at the MP3, MP4, and B3LYP levels have real frequencies. The last two columns of Table IV show some selective frequency results for these structures, for modes compatible with D_{4h} Raman-active modes and with large intensities. As we can see, these frequencies are comparable in magnitude to the experimental results and to the values predicted by MP3, MP4, B3LYP (and MP2) calculations for the corresponding D_{4h} structure. However, both of these structures have a larger number of active modes (with much smaller intensities) than the ones shown in Table IV. Therefore, if we assume that the experiment can detect all Raman-active modes independent of the magnitude of their intensity, we cannot conclude that the experimental measurements support C_{2v} and C_s equally well as the ground-state structure. However, this assumption about the experimental capabilities is not always valid. Very weak vibrations cannot really be resolved or even detected in many cases. Independent of this, an alternative reasonable suggestion, which is put forward here, based on the marginal energy difference between these structures, is that all three isomers coexist and that the experimental values reflect time averages over the three structures.

This picture is consistent with the poor performance of perturbation theory, as was established in Tables II and III. On the other hand, Patterson and Messmer [6,7] have linked the poor convergence of the perturbation expansion with the occurrence of long bonds in Si_{10} and other Si clusters. In this case, the validity of the MP2 (and generally of the perturbation) description could be questionable due to orbitals with small overlaps for which interpair correlation effects are expected to be critical. Therefore relative energies for structures with and without long bonds are not expected to be described by MP2 as accurately as by CCSD(T) or other correlation methods which include, explicitly or implicitly (B3LYP), interpair correlation. Obviously the same is true for the relative energies of structures with (substantially) different numbers of long bonds. As we can see in Fig. 2, the D_{4h} structure has five such long bonds, while the C_s isomer has three and the C_{2v} structure, which is more compact, has only one long bond (the Si_2-Si_3 bond).

The occurrence of long bonds (and its possible consequences) is not the only similarity between Si_6 and Si_{10}. The Si_{10} cluster is also magic and furthermore here too more than one isomer, nearly isoenergetic, is competing for the ground state [7,8]. This could be highly suggestive of a possible connection of the magic property with the occurrence of several isoenergetic isomers competing for the ground state, as a result of the flatness of the energy hypersurface near the minimum. In this respect the stability of the magic clusters would be a dynamic rather than a static property, indirectly related to the Jahn-Teller effect, which is largely responsible for the almost isoenergetic distortions of the higher-symmetry structures. However, before additional and unambiguous supporting evidence becomes available from other magic clusters, this is only a conjecture, which can serve as a working hypothesis for future work.

[1] R. P. Andres *et al.*, J. Mater. Res. **4**, 704 (1989).
[2] K. Raghavachari, Phase Transitions **24-26**, 61 (1990).
[3] M. F. Jarrold, Science **252**, 1085 (1991).
[4] K. Raghavachari, J. Chem. Phys. **84**, 5672 (1986).
[5] E. C. Honea *et al.*, Nature (London) **366**, 42 (1993).
[6] C. H. Patterson and R. P. Messmer, Phys. Rev. B **42**, 7530 (1990).
[7] R. P. Messmer and C. H. Patterson, Chem. Phys. Lett. **192**, 277 (1992).
[8] A. D. Zdetsis (unpublished).
[9] C. Lee, W. Yang, and R. G. Parr, Phys. Rev. B **37**, 785 (1988).
[10] A. D. Becke, J. Chem. Phys. **98**, 5648 (1993).
[11] M. J. Frisch *et al.*, computer code GAUSSIAN 94, revision D.4, Gaussian, Inc., Pittsburgh, PA, 1995.